1 T-Type Calcium Channel

Contents

Main results:

- Estimated number of activation gates for Drosophila T-Type ion channels is 3.
- Modelling the ion channel using Ohmic relationship between current and voltage did not procude good fits to observed current-voltage (I-V) relationship.
- The current-voltage relationship was reproduced when Goldman-Hodgkin-Katz (GHK) voltage flux equation was used instead of Ohmic current
- GHK equation models explicit relationship between current, voltage, temperature and intra-/extracellular ion concentrations.
- The fit of simulated I-V relatoinship to the observed data was improved when the steady-state activation function was shifted along V axis, and corresponding time constant was scaled and shifted along V axis (parameters for shifting and scaling were taken to be free parameters during optimization)

1.1 Model

T-Type Ca^{2+} current was modelled using constant-field equation [5]:

$$I_T(V) = m_T(V)^3 h_T(V) P z^2 \frac{VF^2}{RT} \frac{[Ca^{2+}]_{\text{inside}} - [Ca^{2+}]_{\text{outside}} \exp\left[-zFV/(RT)\right]}{1 - \exp\left[-zFV/(RT)\right]} \tag{1}$$

where m_T and h_T correspond to the activation and inactivation gates, P is the maximum permeability (scaled to either have the current amplitude observed during the electrophysiological experiments reported in [8] (Section 1.3), or to), z is the valence of ion ($= 2$ for Ca^{2+}), V is membrane potential in Volts, F is Faraday's constant ($\approx 9.6485 \times 10^4 C \cdot \text{mol}^{-1}$), R is the universal gas constant ($\approx 8.3145 J/K^\circ \cdot \text{Mol}$), T is temperature is Kelvin (here, $273.16 + 25 = 298.16^\circ$). $[Ca^{2+}]_{\text{inside}}$ and $[Ca^{2+}]_{\text{outside}}$ are the concentrations of Ca^{2+} inside and outside the membrane. The values were set to $23 \times e^{-9}$ and $0.5 \times e^{-3}$ correspondingly, from the motor neurons in Drosophila [4].

Another approach to model the T-Type Ca^{2+} current is by Ohm's law [5, 10]:

$$I_T(V) = g_T m_T(V)^3 h_T(V)(V - V_{Ca}) \tag{2}$$

g_T is the maximum value of the conductance of the T-Type Ca^{2+} current, and V_{Ca} us the reversal potential for Ca^{2+}, which can be estimated given the ion concentrations inside and outside the membrane (see

Section 1.1.1). However, the model with the Ohmic current did not reprocude the I-V relations in [8] correctly (see Sction ...). Similar issue was described in [5], where choosing equation 1 instead of 2 resulted in better fit of the I-V relationship to the experimental data.

1.1.1 Reversal Potential

Reversal potential was estimated by Nernst equation [7]:

$$V_{\text{ion}} = \frac{RT}{zF} \ln \frac{[\text{Ion}]_{\text{outside}}}{[\text{Ion}]_{\text{inside}}}$$

where $[\text{Ion}]_{\text{inside}}$, and $[\text{Ion}]_{\text{outside}}$ are concentrations of the ions (here, Ca^{2+}) inside and outside of the cell. The values for $[Ca^{2+}]_{inside}$ and $[Ca^{2+}]_{outside}$ were taken to be $23nM$, and $0.5mM$ correspondingly from the motor neurons in Drosophila [9]. R is the universal gas constant ($\approx 8.3145 J/K^{\circ} \cdot$ Mol), T is temperature is Kelvin (here, $273.16+25 = 298.16^{\circ}$), F is Faraday's constant ($\approx 9.6485 \times 10^4 C \cdot \text{mol}^{-1}$), z is the valence of the ion ($z = 2$ for Ca^{2+}).

$$V_{Ca} \approx 128mV$$

1.1.2 Activation Gate

Dynamics of the activation variable m_T of T-Type Ca^{2+} channel is given by [10]:

$$\frac{dm_T(V)}{dt} = \frac{m_{T,\infty}(V) - m_T(V)}{\tau_{m_T}(V)}$$

where [1, 10]:

$$m_{T,\infty}(V) = \frac{1}{1 + \exp\left[-(V - V_{m_T,1/2})/k_{m_T}\right]} \tag{3}$$

and

$$\tau_{m_T}(V) = \sigma_{m_T}(V)\tau^{-}_{m_T}(V) + (1 - \sigma_{m_T}(V))\tau^{+}_{m_T}(V) \tag{4}$$

In the equations above, $m_{T,\infty}$ and τ_{m_T} are voltage-sensitive steady-state activation function and time constant, correspondingly. $V_{m_T,1/2}$ is membrane potential at which the steady-state activation function is equal to its half-maximum (i.e. 0.5), and k_{m_T} is the slope factor. $\tau^{-}_{m_T}(V)$ and $\tau^{+}_{m_T}(V)$ describe the time constant below (deactivation) and above (activation) -50mV correspondingly, and $\sigma_{m_T}(V)$ defines smooth transition between the two at -50mV. First, the following functions were fit to the values provided

in [8]:

$$\tau^{-}_{m_T}(V) = 3(a_{m_T,1} + \exp\left[(V - b_{m_T,1})/k_{m_T,1}\right]) \tag{5}$$

$$\tau^{+}_{m_T}(V) = a_{m_T,2} + \exp\left[-(V - b_{m_T,2})/k_{m_T,2}\right] \tag{6}$$

The scaling factor 3 for $\tau^{-}_{m_T}(V)$ is related to the how deactivation time constant was measured in [8] (for the details see Section 1.2.2). As the equations 5 have discontinuity at $V = -50$mV, after fitting the parameters of those equations, the following equation for $\sigma_{m_T}(V)$ was chosen to model smooth transition between the two:

$$\sigma_{m_T}(V) = \frac{1}{1 + \exp\left[c_{\tau_{m,T}}(v + 50)\right]} \tag{7}$$

where $c_{\tau_{m,T}} > 0$ controls the sharpness of the transition and was fitted to the combined activation and deactivation time constants from [8] after fixing the parameters of equation 5.

1.1.3 Inactivation Gate

Inactivation gate was modelled with first-order kinetic scheme [2, 3]:

$$\frac{dh_T(V)}{dt} = \frac{h_{T,\infty}(V) - h(V)}{\tau_{h_T}(V)}$$

where [2, 10]:

$$h_{T,\infty}(V) = \frac{1}{1 + \exp\left[(V - V_{h_T,1/2})/k_{h_T}\right]} \tag{8}$$

and [11]:

$$\tau_{h_T}(V) = h_{T,\infty}(V)(a_{h_T} + \exp\left[(V - b_{h_T})/k_{h_T}\right]) \tag{9}$$

Note 1. Second order kinetic schemes have also been developed for the inactivation gates [10]. The derivation of the equations in the paper are provided in more detail in Section 1.4.3.

1.2 Fitting Data

As the data from the article is not available online, the values were estimated by taking screenshot, importing the image in Coreldraw and estimating the values using visual inspection and coordinate system of Coreldraw. The fitting was performed using python function *scipy.optimize.curve_fit*. The following plots show the estimated activation/inactivation variables, as well as time constants as a function of test potential V, as provided in [8]:

Note 2. The error due to the subjective visual inspection should not be large. I did not estimated the error, but with moving the manually placed dot over the image on the did not have considerable effect in the final values (within the moving range where the manually placed dots were not obviously not overlapping with the ones from the image).

The values of the resulted estimates (plotted in the figures above) are provided in Section 1.4.1.

1.2.1 Estimating Steady-State Activation/Inactivation Function

Parameters for steady-state activation variable were estimated by fitting $m^3_{T,\infty}(V)$ (see Equation 3) to the data from electrophysiological recordings presented in [8] (similar to the procedure described in [1]). The steady-state inactivation was estimated by fitting Equation 8 to the data from the same paper.

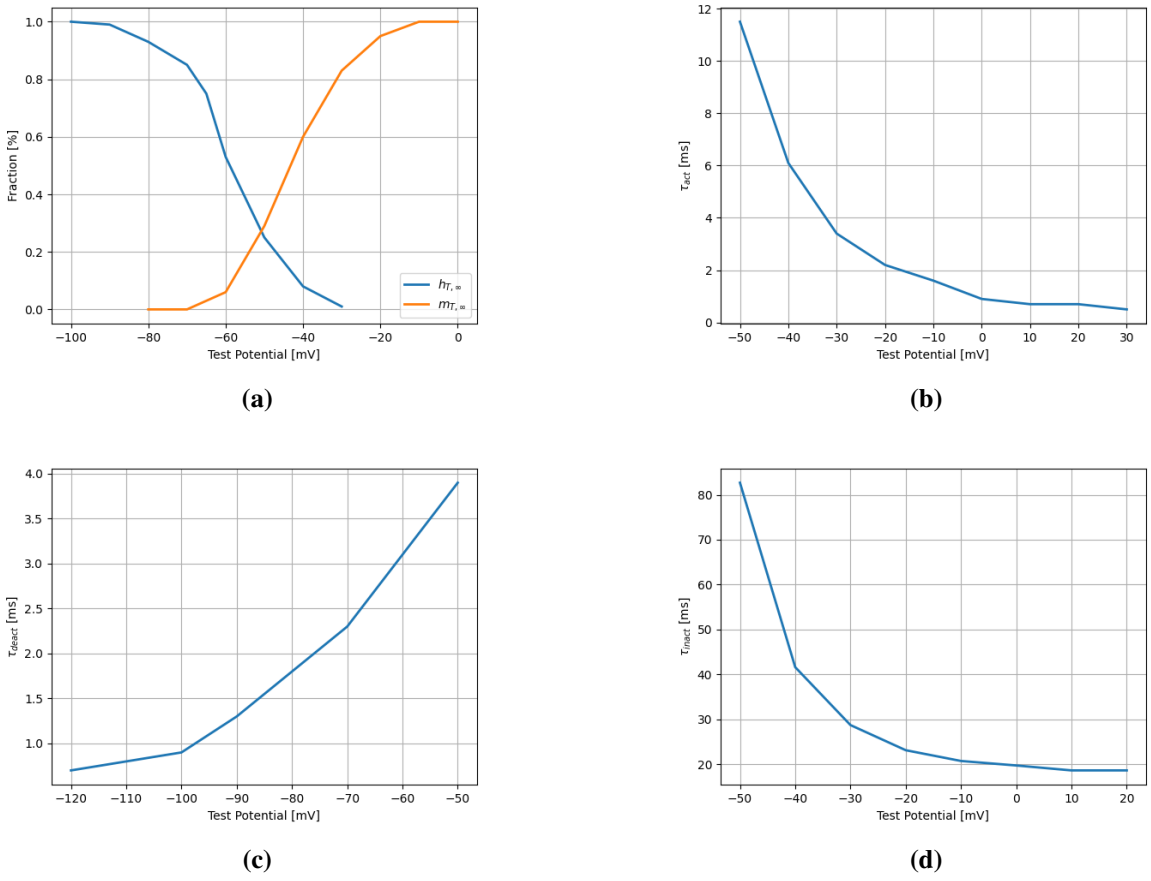

Figure 1: (a) Steady-state activation and inactivation functions of T-type Ca^{2+} channel; (b) Activation, (b) deactivation and (c) inactivation as a functions of test potentials. Data adapted from [8].

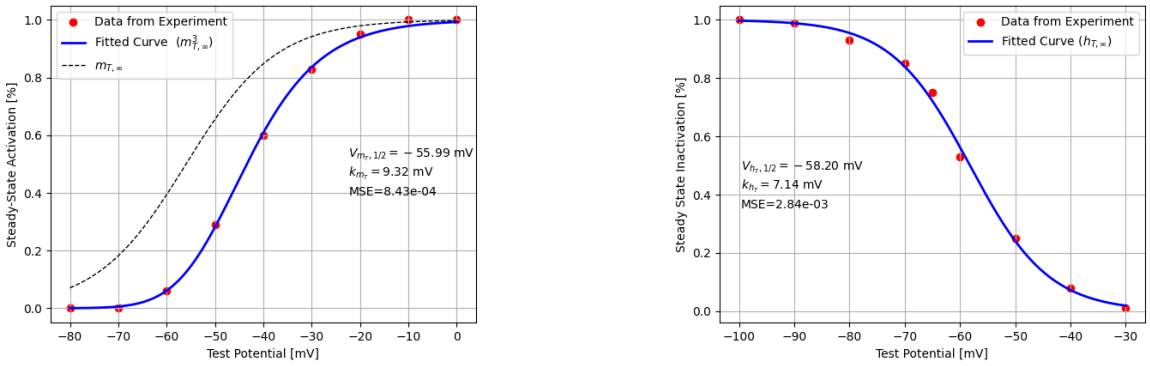

Figure 2: Fitted data to [8].

1.2.2 Estimating Activation/Inactivation Time Constants

The data was taken from [8]. The paper provides information about the values for activation/inactivation variables, as well as time constants as a functions of membrane potentials.

Activation time constant

$a_{T,1}$, $b_{T,1}$, $k_{T,1}$, $a_{T,2}$, $b_{T,2}$, $k_{T,2}$ parameters were fit to the activation ($V \geq -50$ mV) and deactivation ($V < -50$ mV) time constants provided in [8] (equations 5). The initial guess for the parameters were chosen to be 0, -120, 1 for $a_{T,1}$, $b_{T,1}$, $k_{T,1}$, and 0, 50, 1 for $a_{T,2}$, $b_{T,2}$, $k_{T,2}$, correspondingly. The results are shown in Figure 3a.

[8] estimated the activation time constant ($V > -50$ mV) by fitting sum of two exponentials to the recorded current trace. As it is shown in Section 1.4.2, the fitted time constant does not need adjustment to account for the correspondingly time constant of activation. However, the deactivation time constant needs an adjustment.

The authors estimated deactivation time constant by measuring decay of the tail current (τ_{tail}). As the model consists of three activation gates, and closing of each ion channel reuires only one activation gate to close, the deactivation time constant for one gate (out of the three) will be three times as large as τ_{tail} [5]. For this reason, τ_{m_t} for $V < -50$ mV was determined as $3 \times \tau_{\text{tail}}$.

As the set of equations 5 have jump discontinuity at $V = -50$mV, σ_{m_T} was introduced to model a smooth transition between the functions describing the time constant below and above -50mV (equation 7). The parameters of the exponentials modelling activation and deactivation time constants were fixed, and the parameter $c_{\tau_m,T}$ of σ_{m_T} was fitted to the combined data of activation and deactivation time constants from [8] (Figure 3b).

Note 3. Original paper for the base model of the R5 neuron [11] did not model the activation time constant

of T-Type Ca^{2+} channels, as they replaced the activation variable by its steady state equation $m_{t,\infty}(V)$.

Note 4. [2] fitted activation time constant to double exponentials:

$$\tau_{m_T} = a_{\tau_{m_T}} + \frac{b_{\tau_{m_T}}}{\exp\left[(V - V_{\tau^1_{m_T},1/2})/k_{\tau_{m^1_T}}\right] + \exp\left[-(V - V_{\tau^2_{m_T},1/2})/k_{\tau_{m^2_T}}\right]} \tag{10}$$

However, MSE in case of double exponential fit was larger than with fitting the activation time constant with two exponential (see Fig.), as described above.

Inactivation time constant

[8] did not provide experimental values for τ_{h_T} below -50mV. Several authors reported recovery time constant for deinactivation to be much slower than the one of inactivation [2, 5, 6]. Equation 9 is a negative sigmoid, with a left asymtote at $V \approx 216$mV (Figure 4).

Note 5. Another approach would be to fit the time constant only above -50mV and take values below -50mV from another source (e.g. [5]). However, as 1) the values for Drosophila T-Type channel are not available below -50mV, 2) the fitted time constant has the same order of magnitude below -50mV as described in the literature for deinactivation time constant, 3) given the previous comment, the exact velues will only affect time course of the current and is not very relevant for the neuronal model - continuous function was preferred for modelling the inactivation time constant.

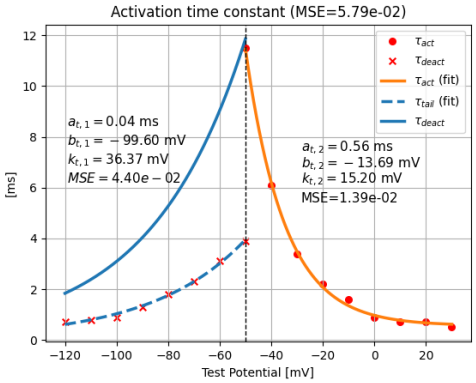

(a) Fitted activation and deactivation time constants using exponential functions

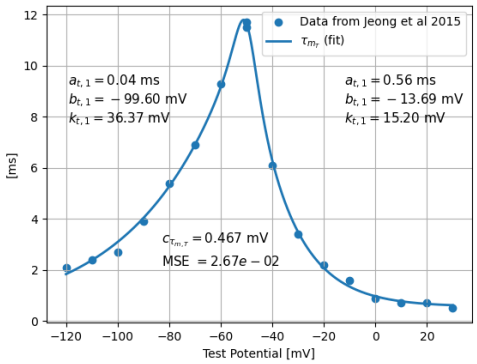

(b) Smooth transition between activation and deactivation time constants

Figure 3: Fitted τ_{m_T} to data from [8].

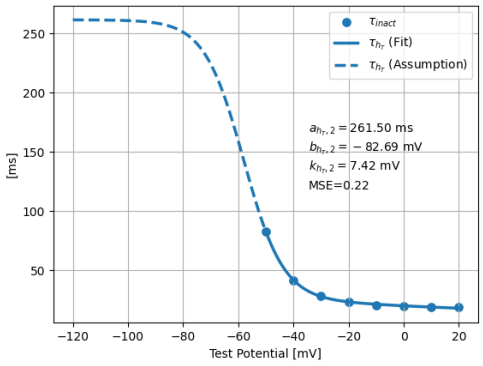

Figure 4: Fitted inactivation time constant

1.3 Simulations of T-Type Ca^{2+} Current

Simulations were done using python package '*scipy.integrate.solve_ivp*' with zero initial conditions. Different integration methods were compared: RK45, BDF, and LSODA. Each solver is optimized for different problems (stiff, non-stiff, etc.). Simulations showed, that for some cases (e.g. simulating only t-type channel) it is best to use RK45. For the simulatins presented in this section, RK45 method was used.

1.3.1 Ohmic Current vs Constant-Field Equation

- How can one fit voltage-current (I-V) relationship?
  - Ohmic current: $I(V) = g(V)(V - V_{ion})$, where $g(V) = \hat{g} m_T(V)^3 h_T(V)$, g is conductance, $\hat{g}$ maximal conductance, $m_T(V)$ ($h_T(V)$) is variable corresponding to activation (inactivation) gate.
  - Constant field equation (also known as Goldman-Hodgkin-Katz (GHK) voltage flux equation): Equation 1
  - The recorded voltage traces and transient I-V relationship to voltage steps is given in Figure 5.
  - Voltage step protocol: The membrane potential was held at holding potential -90 mV, followed by 150ms step pulses that varied from -80-40mV with 10mV increments (see e.g. Figure 6a, second plot from top). The response of the neuron to the voltage steps was recorded (see e.g. Figure 6a, second figure from top).

– Observed I-V relationship was replicated for GHK model, but not for Ohmic current (Figure 6).

Add text, add captions in figure 6.

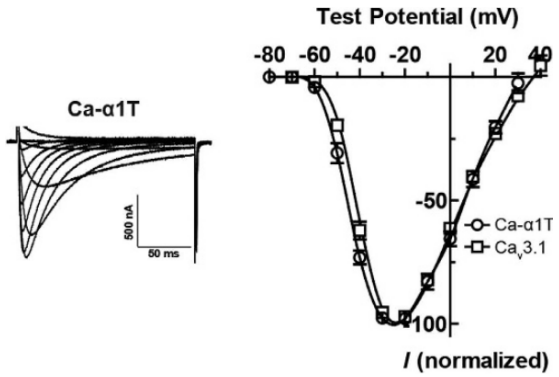

Figure 5: I-V relationship of T-Type Ca^{2+} current in Drosophila. Adapted from [8].

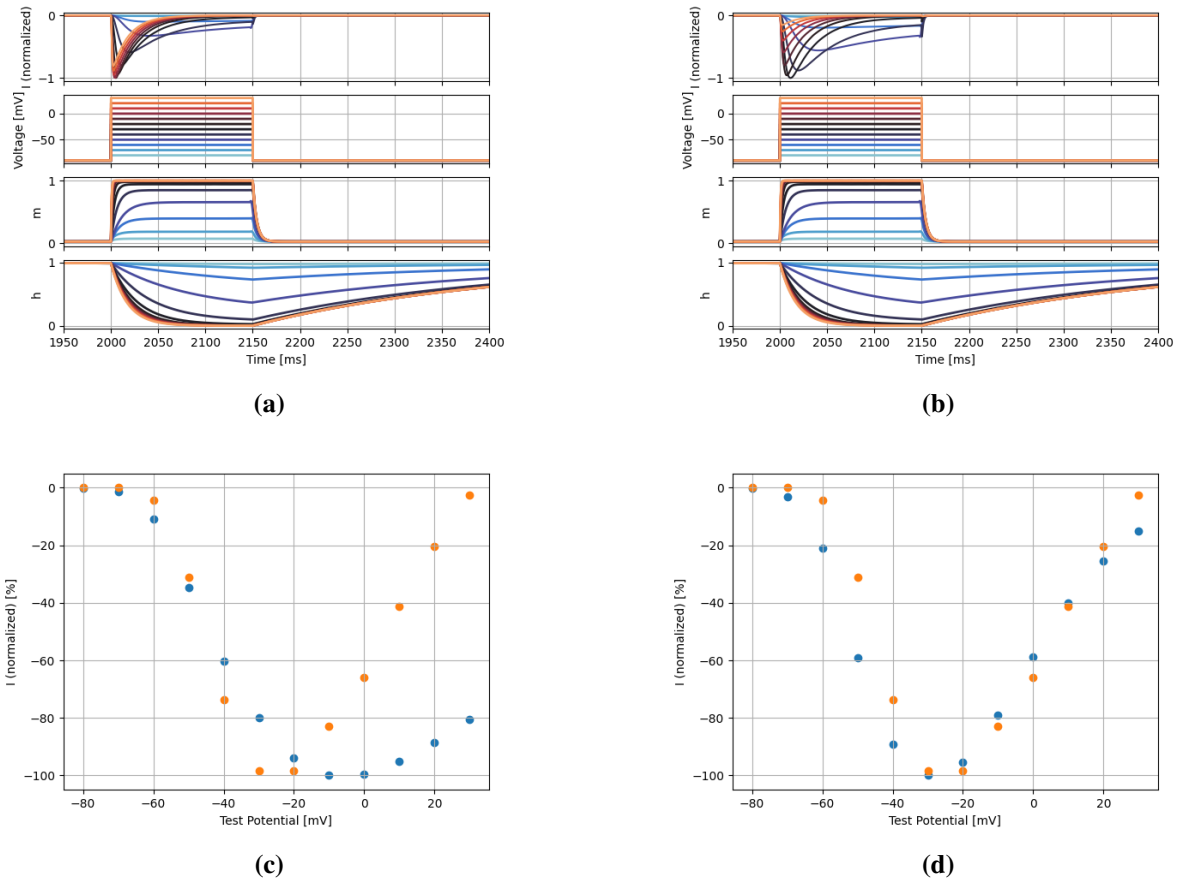

Figure 6: Ohm's low vs constant-field equation for T-Type Ca^{2+} current.

1.3.2 Scaling/Shifting Gating Variables

- $[Ca]_{outside}$, as well as solutions used during voltage-clamp experiments (calcium vs barium, as well as corresponding concentations) affects gating constants, including for mammalian homologes of Drosophila T-Type Ca channels.
- To my knowledge, how exactly the time constants are affected for Drosophila T-Type Ca channels has not been reported.
- For now: shifted steady state activation and scaled tau activation (python function curve_fit with initial guesses p0=[4, 0.5] for shift and scale correspondingly)
- m(v) to m(v-4.95)
- tau to tau*0.45

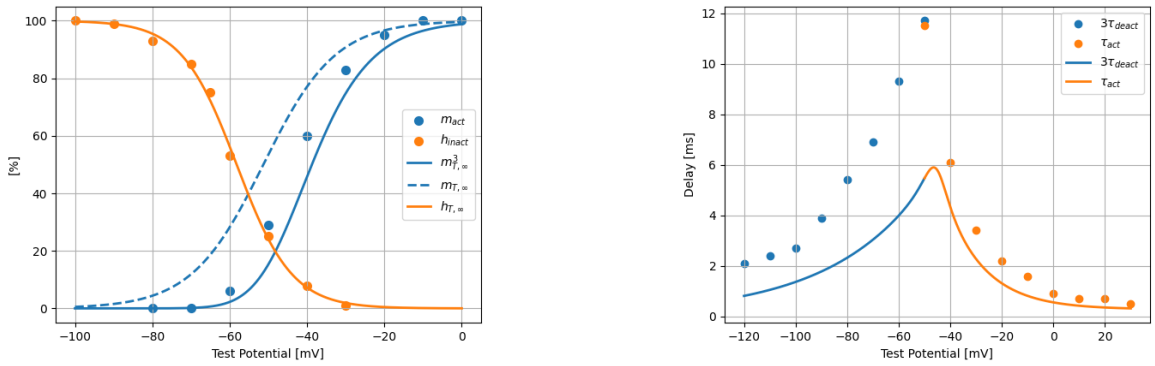

(a) **(b)**

Figure 7: Shifting and scaling time constants of activation gate

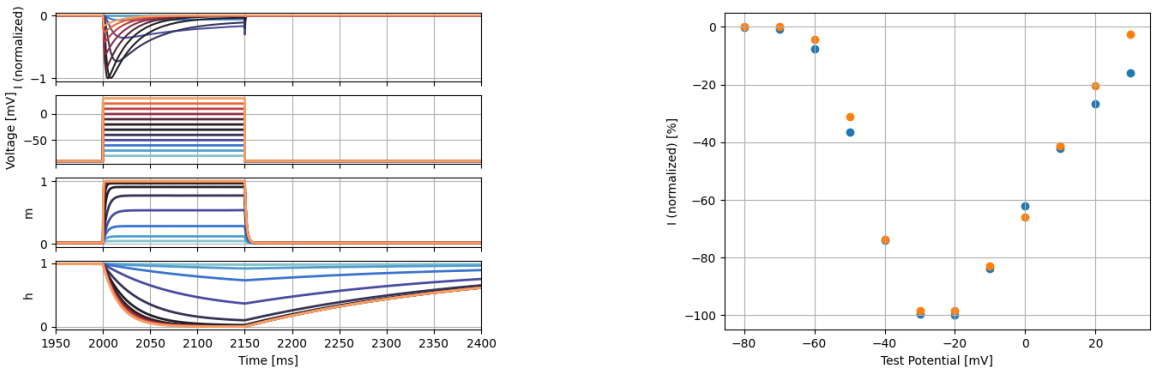

(a) **(b)**

Figure 8: Reconstructed I-V relationship after scaling and shifting activation gate time constant

1.4 Appendix

1.4.1 Estimates of Data in Jeong et al 2015

Inactivation						
Length	y1	y2	Perc	Round	Test Potential	
84.347	138.308	222.656	1.000011856	1	-100	
84.347	138.308	221.91	0.9911674393	0.99	-70	
84.347	138.308	216.864	0.931343142	0.93	-80	
84.347	138.308	210.296	0.8534743382	0.85	-70	
84.347	138.308	201.258	0.7463217423	0.75	-65	
84.347	138.308	183.423	0.5348737952	0.53	-60	
84.347	138.308	159.321	0.2491256358	0.25	-50	
84.347	138.308	145.041	0.0798250086	0.08	-40	
84.347	138.308	139.015	0.008382040855	0.01	-30	

Activation						
Length	y1	y2	Perc	Round	Test Potential	
84.347	138.308	138.308	0	0	-80	
84.347	138.308	138.308	0	0	-70	
84.347	138.308	143.029	0.05597116673	0.06	-60	
84.347	138.308	162.76	0.2898976846	0.29	-50	
84.347	138.308	189.012	0.6011357843	0.6	-40	
84.347	138.308	208.417	0.8311973159	0.83	-30	
84.347	138.308	218.852	0.954912445	0.95	-20	
84.347	138.308	222.256	0.9952695413	1	-10	
84.347	138.308	222.656	1.000011856	1	0	

Tau Activation						
Test Potential	length	k	y1	y2	Tau	Round
-50	94.853	10	110.837	220.142	11.52362076	11.5
-40	94.853	10	110.837	168.638	6.093745058	6.1
-30	94.853	10	110.837	143.507	3.444276934	3.4
-20	94.853	10	110.837	131.792	2.209207932	2.2
-10	94.853	10	110.837	126.028	1.60153079	1.6
0	94.853	10	110.837	119.373	0.8999188218	0.9
10	94.853	10	110.837	117.386	0.6904367811	0.7
20	94.853	10	110.837	117.187	0.6694569492	0.7
30	94.853	10	110.837	115.995	0.5437888101	0.5

Tau Inactivation						
Test Potential	length	k	y1	y2	Tau	Round
-50	122.173	100	120.28	221.365	82.73923044	82.7
-40	122.173	100	120.28	171.102	41.59838917	41.6
-30	122.173	100	120.28	155.338	28.69537459	28.7
-20	122.173	100	120.28	148.484	23.08529708	23.1
-10	122.173	100	120.28	145.514	20.65431806	20.7
0	122.173	100	120.28	144.372	19.71957798	19.7
10	122.173	100	120.28	143.001	18.59739877	18.6
20	122.173	100	120.28	143.001	18.59739877	18.6

Tau Deactivation						
Test Potential	length	k	y1	y2	Tau	Round
-120	130.684	5	125.975	143.595	0.6741452664	0.7
-110	130.684	5	125.975	146.32	0.7784043953	0.8
-100	130.684	5	125.975	149.948	0.9172125126	0.9
-90	130.684	5	125.975	158.758	1.254285146	1.3
-80	130.684	5	125.975	173.788	1.829336415	1.8
-70	130.684	5	125.975	186.399	2.311836185	2.3
-60	130.684	5	125.975	206.439	3.07857121	3.1
-50	130.684	5	125.975	227.86	3.898143614	3.9

1.4.2 From Current Trace to Sum of Exponentials

Sum of exponentials and gating time constants

$$\frac{dm}{dt} = \frac{m_\infty - m}{\tau_m} \; , \; \frac{dh}{dt} = \frac{h_\infty - h}{\tau_h} \qquad (1)$$

$$I(t) = g\, m^p h\, (V - E) \qquad (2)$$

$$\left.\begin{array}{l} m(0) = h(0) = 0 \\ p = 3 \end{array}\right\} \Rightarrow \left.\begin{array}{l} m(t) = m_\infty \left(1 - e^{-t/\tau_m}\right) \\ h(t) = h_\infty \left(1 - e^{-t/\tau_h}\right) \end{array}\right\} \Rightarrow$$

(2)

$$\Rightarrow I(t) = g\, m_\infty^3 \left(1 - e^{-t/\tau_m}\right)^3 h_\infty \left(1 - e^{-t/\tau_h}\right)(V - E) =$$

$$= g\, m_\infty^3 \left(1 - e^{-3t/\tau_m} - 3e^{-t/\tau_m} + 3e^{-2t/\tau_m}\right) h_\infty \left(1 - e^{-t/\tau_h}\right)(V - E) \simeq$$

$$\simeq g\, m_\infty^3 \left(1 - 3e^{-t/\tau_m}\right) h_\infty \left(1 - e^{-t/\tau_h}\right)(V - E) =$$

$$= g\, m_\infty^3 h_\infty \left(1 - e^{-t/\tau_h} - 3e^{-t/\tau_m} + e^{-t/\tau_m - t/\tau_h}\right)(V - E) \simeq$$

$$\simeq g\, m_\infty^3 h_\infty \left(1 - e^{-t/\tau_h} - 3e^{-t/\tau_m}\right)(V - E) =$$

$$= \underbrace{g\, m_\infty^3 h_\infty (V - E)}_{\text{Steady state term}} \underbrace{- g\, m_\infty^3 h_\infty (V - E) e^{-t/\tau_h} - 3 g\, m_\infty^3 h_\infty (V - E) e^{-t/\tau_m}}_{\text{Transient term}}$$

$$I_{transient}(t) = A_1 e^{-t/\tau_m} + A_2 e^{-t/\tau_h}$$

$$A_1 = -3 g\, m_\infty^3 h_\infty (V - E)$$

$$A_2 = -g\, m_\infty^3 h_\infty (V - E)$$

← Thus, τ_m and τ_h can be directly fitted by recorded transient currents $I_{transient}$

1.4.3 Derivation of equations in Wang 1991

$$\frac{dh}{dt} = \alpha_1 (1 - h - d) - \beta_1 h \qquad (1)$$

$$\frac{dd}{dt} = \beta_2 (1 - h - d) - \alpha_2 d \qquad (2)$$

steady state

$$\alpha_1 (1 - h_\infty - d_\infty) = \beta_1 h_\infty \;) \Rightarrow \alpha_1 (1 - d_\infty) = h_\infty (\alpha_1 + \beta_1) \Rightarrow h_\infty = \frac{\alpha_1 (1 - d_\infty)}{\alpha_1 + \beta_1}$$

$$\beta_2 (1 - h_\infty - d_\infty) = \alpha_2 d_\infty \;) \Rightarrow \beta_2 \left(1 - \frac{\alpha_1 (1 - d_\infty)}{\alpha_1 + \beta_1} - d_\infty\right) = \alpha_2 d_\infty$$

$$1 - \frac{\alpha_1 - \alpha_1 d_\infty + \alpha_1 d_\infty + \beta_1 d_\infty}{\alpha_1 + \beta_1} = \frac{\alpha_2}{\beta_2} d_\infty$$

$$\frac{\alpha_1 + \beta_1 d_\infty}{\alpha_1 + \beta_1} = 1 - \frac{\alpha_2}{\beta_2} d_\infty \;) \Rightarrow \alpha_1 + \beta_1 d_\infty = \alpha_1 + \beta_1 - \frac{\alpha_2 (\alpha_1 + \beta_1)}{\beta_2} d_\infty$$

$$d_\infty \left(\beta_1 + (\alpha_1 + \beta_1) \frac{\alpha_2}{\beta_2} \right) = \beta_1$$

$$d_\infty \cdot \frac{\beta_1 \beta_2 + \alpha_1 \alpha_2 + \alpha_2 \beta_1}{\beta_2} = \beta_1$$

$$d_\infty = \frac{\beta_1 \beta_2}{\beta_1 \beta_2 + \alpha_2 (\alpha_1 + \beta_1)}$$

$$\beta_1 = \alpha_1 K_1$$

$$\beta_2 = \alpha_2 K_2$$

$$\Rightarrow d_\infty = \frac{\alpha_1 K_1 \alpha_2 K_2}{\alpha_1 K_1 \alpha_2 K_2 + \alpha_2 (\alpha_1 + \alpha_1 K_1)} =$$

$$= \frac{\alpha_1 K_1 K_2}{\alpha_1 K_1 K_2 + \alpha_1 (1 + K_1)} = \frac{K_1 K_2}{K_1 K_2 + 1 + K_1} = \frac{K_1 K_2}{1 + K_1 (1 + K_2)}$$

$$h_\infty = \frac{\alpha_1(1-d_\infty)}{\alpha_1+\beta_1} = \frac{\alpha_1}{\alpha_1+K_1\alpha_1}\left(1-\frac{K_1K_2}{1+K_1+K_1K_2}\right) =$$

$$= \frac{1}{1+K_1}\cdot\frac{1+K_1+K_1K_2-K_1K_2}{1+K_1+K_1K_2} = \frac{1}{1+K_1}\cdot\frac{1+K_1}{1+K_1+K_1K_2} =$$

$$= \frac{1}{1+K_1(1+K_2)}$$

$$\boxed{\begin{aligned} h_\infty &= \frac{1}{1+K_1(1+K_2)} \\ d_\infty &= K_1K_2\,h_\infty \end{aligned}} \qquad (A2a) \quad (A2b)$$

$$K_1 = K_2 \Rightarrow \boxed{\begin{aligned} h_\infty &= \frac{1}{1+K+K^2} \\ d_\infty &= K^2 h_\infty \end{aligned}} \qquad (A3)$$

---

(1), (2) $\rightarrow$

$$\frac{d}{dt}\begin{pmatrix} h \\ d \end{pmatrix} = \begin{pmatrix} -\alpha_1-\beta_1 & -\alpha_1 \\ -\beta_2 & -\alpha_2-\beta_2 \end{pmatrix}\begin{pmatrix} h \\ d \end{pmatrix} + \begin{pmatrix} \alpha_1 \\ \beta_2 \end{pmatrix}$$

Associated homogeneous equation:

$$\frac{d}{dt}\begin{pmatrix} h \\ d \end{pmatrix} = \begin{pmatrix} -\alpha_1-\beta_1 & -\alpha_1 \\ -\beta_2 & -\alpha_2-\beta_2 \end{pmatrix}\begin{pmatrix} h \\ d \end{pmatrix} \qquad \begin{pmatrix} h \\ d \end{pmatrix} \equiv \vec{x}$$

$$\begin{pmatrix} -\alpha_1-\beta_1 & -\alpha_1 \\ -\beta_2 & -\alpha_2-\beta_2 \end{pmatrix} \equiv A$$

$\lambda' = -\lambda$ ← eigenvalues

$$\vec{x}' = A\vec{x}$$

$$\det(A + \lambda I) = \det\begin{pmatrix} -\alpha_1 - \beta_1 + \lambda & -\alpha_1 \\ -\beta_2 & -\alpha_2 - \beta_2 + \lambda \end{pmatrix} =$$

$$= (-\alpha_1 - \beta_1 + \lambda)(-\alpha_2 - \beta_2 + \lambda) - \alpha_1\beta_2 =$$

$$= \alpha_1\alpha_2 + \alpha_1\beta_2 - \lambda\alpha_1 + \alpha_2\beta_1 + \beta_1\beta_2 - \lambda\beta_1 - \lambda\alpha_2 - \lambda\beta_2 + \lambda^2 - \alpha_1\beta_2 =$$

$$= \lambda^2 + \lambda\underbrace{(-\alpha_1 - \beta_1 - \alpha_2 - \beta_2)}_{Tr} + \underbrace{\alpha_1\alpha_2 + \beta_1(\alpha_2 + \beta_2)}_{\mathcal{D}} =$$

$$= \lambda^2 + Tr\cdot\lambda + \mathcal{D}$$

$$Tr = -(\alpha_1 + \beta_1 + \alpha_2 + \beta_2) = -\left(\frac{1}{\tau_1} + \frac{1}{\tau_2}\right)$$

$$\mathcal{D} = \alpha_1\alpha_2 + \beta_1(\alpha_2 + \beta_2) = \alpha_1\alpha_2 + K\alpha_1(\alpha_2 + K\alpha_2) =$$

$$= \alpha_1\alpha_2(1 + K(1+K))$$

$$K_1 = \frac{\beta_1}{\alpha_1} \Rightarrow \quad \beta_1 = K_1\alpha_1$$

$$\tau_1 = \frac{1}{\alpha_1 + \beta_1} \Rightarrow \tau_1 = \frac{1}{\alpha_1(1+K_1)} \Rightarrow \quad \alpha_1 = \frac{1}{\tau_1(1+K_1)}$$

$$\text{similarly: } \alpha_2 = \frac{1}{\tau_2(1+K_2)}$$

$$\Rightarrow \quad \mathcal{D} = \frac{1 + K(1+K)}{\tau_1\tau_2(1+K)^2}$$

$$\lambda_1, \lambda_2 = \frac{1}{2}\left[-T_r \pm \sqrt{T_r^2 - 4D} \right]$$

$$T_r^2 - 4D = \left(\frac{1}{\tau_1} + \frac{1}{\tau_2}\right)^2 - \frac{4(1+K(1+K))}{\tau_1\tau_2(1+K)^2} =$$

$$= \left(\frac{1}{\tau_1} - \frac{1}{\tau_2}\right)^2 + \frac{4}{\tau_1\tau_2} - \frac{4(1+K(1+K))}{\tau_1\tau_2(1+K)^2} = \left(\frac{1}{\tau_1} - \frac{1}{\tau_2}\right)^2 + \frac{4(1+K)^2 - 4 - 4K - 4K^2}{\tau_1\tau_2(1+K)^2} =$$

$$= \left(\frac{1}{\tau_1} - \frac{1}{\tau_2}\right)^2 + \frac{4 + 8K + 4K^2 - 4 - 4K - 4K^2}{\tau_1\tau_2(1+K)^2} = \left(\frac{1}{\tau_1} - \frac{1}{\tau_2}\right)^2 + \frac{4K}{\tau_1\tau_2(1+K)^2}$$

$$\lambda_1, \lambda_2 = \frac{1}{2}\left[\left(\frac{1}{\tau_1} + \frac{1}{\tau_2}\right) \pm \sqrt{\left(\frac{1}{\tau_1} - \frac{1}{\tau_2}\right)^2 + \frac{4K}{\tau_1\tau_2(1+K)^2}} \right]$$

(from the paper)

$$\tau_1^{-1}, \tau_2^{-1} = \frac{1}{2}\left[(\lambda_1 + \lambda_2) \pm \sqrt{(\lambda_1 + \lambda_2)^2 - \frac{4(1+K)^2\lambda_1\lambda_2}{1+K(1+K)}} \right]$$

Measurable time constants in experiments are λ_1^{-1} and λ_2^{-1} (i.e. τ_R and τ_r).

general solution for d and h:

$$A_0^{(\ell)} + A_1^{(\ell)} \exp(-\lambda_1 t) + A_2^{(\ell)} \exp(-\lambda_2 t)$$

where $\ell = \{d, h\}$

Approximations:

$$\tilde{\tau}_1 \simeq \lambda_1^{-1}$$

$$\tilde{\tau}_2 \simeq \lambda_2^{-1}\left[1+K(1+K)\right]/(1+K)^2$$

$$\dot{h} = \alpha_1(1-h-d) - \beta_1 h \qquad (1)$$

$$\dot{d} = \beta_2(1-h-d) - \alpha_2 d \qquad (2)$$

As (1) describes much faster process than (2), the authors used rapid equilibrium hypothesis on the former: assume steady state $\frac{dh}{dt}=0$. Then:

$$h = \frac{\alpha_1(1-d)}{\alpha_1+\beta_1} \quad (2) \Rightarrow$$

$$\Rightarrow \quad \dot{d} = \beta_2\left(1 - \frac{\alpha_1(1-d)}{\alpha_1+\beta_1} - d\right) - \alpha_2 d =$$

$$= \beta_2 - \frac{\alpha_1\beta_2(1-d)}{\alpha_1+\beta_1} - \beta_2 d - \alpha_2 d =$$

$$= \frac{\alpha_1\beta_2 + \beta_1\beta_2 - \alpha_1\beta_2 + \alpha_1\beta_2 d - \alpha_1\beta_2 d - \beta_1\beta_2 d - \alpha_1\alpha_2 d - \alpha_2\beta_1 d}{\alpha_1+\beta_1} =$$

$$= \frac{\alpha_1\alpha_2 K^2(1-d) - \alpha_1\alpha_2 d - \alpha_1\alpha_2 K d}{\alpha_1+\beta_1}$$

$$\dot{d} = \frac{\alpha_1\alpha_2 K^2(1-d) - \alpha_1\alpha_2 d - \alpha_1\alpha_2 K d}{\alpha_1 + \alpha_1 K} =$$

$$= \frac{\alpha_2 K^2(1-d) - \alpha_2 d - \alpha_2 K d}{1+K} = \frac{\alpha_2\left(K^2 - K^2 d - d - Kd\right)}{1+K} =$$

$$= \frac{\alpha_2\left[K^2 - d\left(1 + K(1+K)\right)\right]}{1+K} = -\frac{\alpha_2\left(1+K(1+K)\right)}{1+K} d + \frac{\alpha_2 K^2}{1+K}.$$

$$\frac{1+K}{\alpha_2\left(1+K(1+K)\right)}\dot{d} = -d + \frac{\alpha_2 K^2}{1+K} \cdot \frac{1+K}{\alpha_2\left(1+K(1+K)\right)}$$

$$\frac{1+K}{\alpha_2\left(1+K(1+K)\right)} \equiv \lambda_2^{-1}$$

$$\boxed{\lambda_2^{-1}\dot{d} = -d + \frac{K^2}{1+K(1+K)}} \quad (*)$$

$$\alpha_1 = \frac{1}{\tau_1(1+K_1)}$$

$$\left.\begin{aligned} \lambda_2^{-1} &= \frac{1+K}{\alpha_2\left(1+K(1+K)\right)} \\ \alpha_2 &= \frac{1}{\tau_2(1+K)} \end{aligned}\right\} \Rightarrow \lambda_2^{-1} = \frac{\tau_2(1+K)^2}{1+K(1+K)}$$

$$\boxed{\tau_2 = \frac{\lambda_2^{-1}\left(1+K(1+K)\right)}{(1+K)^2}}$$

1.4.4 Overcoming Singularities in Constant-Field Equation

$$I_T = \hat{g}\, P\, z^2\, \frac{EF^2}{RT}\, \frac{[C_a^{2+}]_i - [Ca^{2+}]_o \exp(-zFE/RT)}{1 - \exp(-zFE/RT)}$$

$\hat{g} = m^3 h$

if $-\frac{zFE}{RT} \gg 1$ $\Rightarrow$ $I_T = \hat{g}\, P\, z^2\, \frac{EF^2}{RT} \cdot \frac{-[C_a^{2+}]_o}{0 - 1}$

$$I_T = \hat{g}\, P\, z^2\, \frac{EF^2}{RT} [C_a^{2+}]_o$$

if $E=0$ $\Rightarrow$ $I_T \approx \hat{g}\, P\, z^2\, \frac{EF^2}{RT}\, \frac{[C_a^{2+}]_i - [C_a^{2+}]_o \left(1 - \frac{zFE}{RT}\right)}{1 - \left(1 - \frac{zFE}{RT}\right)} \simeq$

$$\simeq \hat{g}\, P\, z^2\, \frac{EF^2}{RT}\, \frac{[C_a^{2+}]_i - [C_a^{2+}]_o}{\frac{zFE}{RT}}$$

$$I_T = \hat{g}\, P\, z F \left([C_a^{2+}]_i - [C_a^{2+}]_o\right)$$

1.4.5 Additional Figures

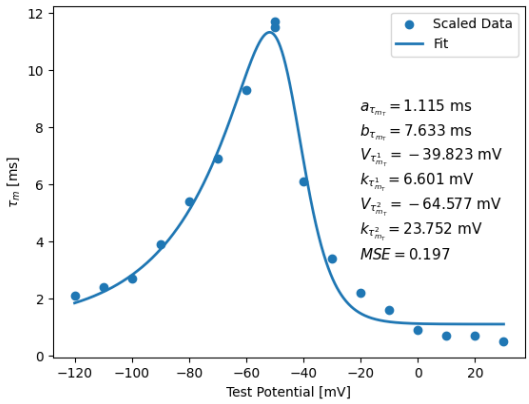

Figure 9: Fitting time constant of activation function for T-Type Ca^{2+} channel by double exponential function (Eq. 10). The fitting was done using the Python library *scipy.optimize.curve_fit* with the following initial guesses for the parameters: $a_{\tau_{m_T}} = 2$, $b_{\tau_{m_T}} = 1$, $V_{\tau^1_{m_T}} = -100$, $k_{\tau^1_{m_T}} = 10$, $V_{\tau^2_{m_T}} = -40$, $k_{\tau^2_{m_T}} = 10$.

References

1. Coulter, D. A., Huguenard, J. R. & Prince, D. A. Calcium Currents in Rat Thalamocortical Relay Neurones: Kinetic Properties of the Transient, Low-Threshold Current. *The Journal of Physiology* **414,** 587–604. ISSN: 0022-3751. PMID: 2607443 (July 1989).

2. Destexhe, A., Contreras, D., Steriade, M., Sejnowski, T. J. & Huguenard, J. R. In Vivo, in Vitro, and Computational Analysis of Dendritic Calcium Currents in Thalamic Reticular Neurons. *The Journal of Neuroscience: The Official Journal of the Society for Neuroscience* **16,** 169–185. ISSN: 0270-6474. PMID: 8613783 (Jan. 1996).

3. Destexhe, A., Mainen, Z. F. & Sejnowski, T. J. Synthesis of Models for Excitable Membranes, Synaptic Transmission and Neuromodulation Using a Common Kinetic Formalism. *Journal of Computational Neuroscience* **1,** 195–230. ISSN: 0929-5313, 1573-6873. http://link.springer.com/10.1007/BF00961734 (2024) (Aug. 1994).

4. Frankenhaeuser, B. & Hodgkin, A. L. The Action of Calcium on the Electrical Properties of Squid Axons. *The Journal of Physiology* **137,** 218–244. ISSN: 0022-3751. PMID: 13449874 (July 11, 1957).

5. Huguenard, J. R. & McCormick, D. A. Simulation of the Currents Involved in Rhythmic Oscillations in Thalamic Relay Neurons. *Journal of Neurophysiology* **68,** 1373–1383. ISSN: 0022-3077, 1522-1598. https://www.physiology.org/doi/10.1152/jn.1992.68.4.1373 (2024) (Oct. 1, 1992).

6. Huguenard, J. R. & Prince, D. A. A Novel T-type Current Underlies Prolonged Ca(2+)-Dependent Burst Firing in GABAergic Neurons of Rat Thalamic Reticular Nucleus. *The Journal of Neuroscience: The Official Journal of the Society for Neuroscience* **12,** 3804–3817. ISSN: 0270-6474. PMID: 1403085 (Oct. 1992).

7. Izhikevich, E. M. *Dynamical Systems in Neuroscience: The Geometry of Excitability and Bursting* ISBN: 978-0-262-27607-8. https://direct.mit.edu/books/book/2589/Dynamical-Systems-in-NeuroscienceThe-Geometry-of (2024) (The MIT Press, July 21, 2006).

8. Jeong, K. *et al.* Ca-a1T, a Fly T-type Ca2+ Channel, Negatively Modulates Sleep. *Scientific Reports* **5,** 17893. ISSN: 2045-2322. PMID: 26647714. https://www.nature.com/articles/srep17893 (Dec. 9, 2015).

9. Macleod, G. T., Hegström-Wojtowicz, M., Charlton, M. P. & Atwood, H. L. Fast Calcium Signals in *Drosophila* Motor Neuron Terminals. *Journal of Neurophysiology* **88,** 2659–2663. ISSN: 0022-3077, 1522-1598. https://www.physiology.org/doi/10.1152/jn.00515.2002 (2024) (Nov. 1, 2002).

10. Wang, X. J., Rinzel, J. & Rogawski, M. A. A Model of the T-type Calcium Current and the Low-Threshold Spike in Thalamic Neurons. *Journal of Neurophysiology* **66,** 839–850. ISSN: 0022-3077, 1522-1598. https://www.physiology.org/doi/10.1152/jn.1991.66.3.839 (2024) (Sept. 1, 1991).

11. Wang, X.-J. Multiple Dynamical Modes of Thalamic Relay Neurons: Rhythmic Bursting and Intermittent Phase-Locking. *Neuroscience* **59,** 21–31. ISSN: 03064522. https://linkinghub.elsevier.com/retrieve/pii/0306452294900957 (2024) (Mar. 1994).